

Degradation of *trans*-ferulic acid in acidic aqueous medium by anodic oxidation, electro-Fenton and photoelectro-Fenton

Nelly Flores, Ignasi Sirés, José Antonio Garrido, Francesc Centellas, Rosa María Rodríguez, Pere Lluís Cabot, Enric Brillas*

Laboratori d'Electroquímica dels Materials i del Medi Ambient, Departament de Química Física, Facultat de Química, Universitat de Barcelona, Martí i Franquès 1-11, 08028 Barcelona, Spain

Article submitted for publication in Journal of Hazardous Materials

* Corresponding author: Tel.: +34 934021223; fax: +34 934021231

E-mail address: brillas@ub.edu (E. Brillas)

Abstract

Solutions of pH 3.0 containing *trans*-ferulic acid, a phenolic compound in olive oil mill wastewater, have been comparatively degraded by anodic oxidation with electrogenerated H₂O₂ (AO-H₂O₂), electro-Fenton (EF) and photoelectro-Fenton (PEF). Trials were performed with a BDD/air-diffusion cell, where oxidizing •OH was produced from water discharge at the BDD anode and/or in the solution bulk from Fenton's reaction between cathodically generated H₂O₂ and added catalytic Fe²⁺. The substrate was very slowly removed by AO-H₂O₂, whereas it was very rapidly abated by EF and PEF, at similar rate in both cases, due to its fast reaction with •OH in the bulk. The AO-H₂O₂ process yielded a slightly lower mineralization than EF, which promoted the accumulation of barely oxidizable products like Fe(III) complexes. In contrast, the fast photolysis of these latter species under irradiation with UVA light in PEF led to an almost total mineralization with 98% total organic carbon decay. The effect of current density and substrate concentration on the performance of all treatments was examined. Several solar PEF (SPEF) trials showed its viability for the treatment of wastewater containing *trans*-ferulic acid at larger scale. Four primary aromatic products were identified by GC-MS analysis of electrolyzed solutions, and final carboxylic acids like fumaric, acetic and oxalic were detected by ion-exclusion HPLC. A reaction sequence for *trans*-ferulic acid mineralization involving all the detected products is finally proposed.

Keywords: Anodic oxidation; Electro-Fenton; Oxidation products; Photoelectro-Fenton; *trans*-Ferulic acid

1. Introduction

The olive oil industry in Mediterranean countries like Spain, Italy, Greece and Portugal supplies about 77% of the worldwide output of this product. During the extraction of the olive oil, however, a volume of industrial effluents as large as 30 million cubic meters is produced annually in the world. Olive oil mill wastewater (OOMWW) has acidic pH near 5, high chemical and biochemical oxygen demand up to 110 g L⁻¹ and 170 g L⁻¹, respectively, and total solids contents up to 150 g L⁻¹ [1], which is very harmful for the environment by the negative effects over soil microbial population [2] and aquatic ecosystems [3]. Phenols, lipids, sugars and tannins are the main organic components of OOMWW, representing up to 37% of the total mass [4,5]. One of the most important phenolic compounds is *trans*-ferulic acid (4-hydroxy-3-methoxycinnamic acid), much more abundant than its *cis* isomer. *trans*-Ferulic acid is also present in the plant cell wall of various fruits and vegetables, possesses a high antioxidant activity and low toxicity after oral administration (LD₅₀ = 3200 mg kg⁻¹) and has been detected in rivers, lakes and sea sediments [6]. At industrial level, it is used as ingredient in many drug formulations and food additives, being its derivative vanillin of huge commercial importance in the food industry [7]. So far, little information about the degradation of *trans*-ferulic acid for wastewater treatment is available. Several authors have described its oxidation by pyrilium salt photosensitized with sunlight [8] and advanced oxidation processes (AOPs) such as catalytic wet oxidation [9], heterogeneous Fenton [10] and TiO₂ photocatalysis [11], but the use of powerful electrochemical AOPs (EAOPs) for treating water polluted with *trans*-ferulic acid has not yet been reported.

Over the last two decades, EAOPs have received growing attention for the remediation of wastewater contaminated with biorecalcitrant organics [12-16]. The common feature of these methods is the in situ generation of reactive oxygen species (ROS) such as hydroxyl radical ($\bullet\text{OH}$), which can attack most organics up to their mineralization (conversion into CO₂ and inorganic ions) due to its high standard reduction potential ($E^\circ = 2.80 \text{ V/SHE}$). The most popular EAOP is anodic

oxidation (AO), also so-called electrochemical oxidation. In AO, a high current density (j) is usually applied to the anode M of the cell to produce oxidizing physisorbed hydroxyl radical $M(\bullet\text{OH})$ as intermediate of water discharge to O_2 at the anode surface by reaction (1) [12,17-19]:



When considering the abatement of aromatic organics and even carboxylic acids, the physisorbed BDD($\bullet\text{OH}$) generated at boron-doped diamond (BDD) anode has higher oxidation ability than $M(\bullet\text{OH})$ produced by other common anodes [20-23]. This is due to the larger O_2 -overpotential of BDD and the low interaction between its surface and $\bullet\text{OH}$, which favors its reaction with organics [12]. At present, the BDD electrode is the preferred anode for AO.

When an undivided cell is used with a carbonaceous cathode able to electrogenerate H_2O_2 , the process is called AO- H_2O_2 , where organics are preferentially destroyed by physisorbed $M(\bullet\text{OH})$ along with a minor participation of other ROS such as H_2O_2 and its anodic oxidation product $\text{HO}_2\bullet$ [13,14]. It is well-known that H_2O_2 can be efficiently formed from the two-electron reduction of O_2 gas via reaction (2) at cathodes such as activated carbon fiber [24], carbon nanotubes [25,26], graphite felt [27], carbon modified with metals or metal oxides nanoparticles [28], carbon felt [29-31], carbon-polytetrafluoroethylene (PTFE) O_2 or air-diffusion [32-34], and BDD [35,36].



Another widely used EAOP is the electro-Fenton (EF) process, where a catalytic amount of Fe^{2+} is added to the solution to enhance the oxidation power of H_2O_2 via Fenton's reaction (3) with production of Fe^{3+} and $\bullet\text{OH}$ in the bulk [29-34]. The optimum pH for EF is ~ 3 and organic pollutants are then destroyed by both kinds of ROS, $M(\bullet\text{OH})$ and $\bullet\text{OH}$. In our laboratory, we have been developing other EAOPs like UVA photoelectro-Fenton (PEF) or solar PEF (SPEF) in which the treated solution is irradiated with either artificial UVA light or sunlight, respectively [37-40].

This radiation causes the photoreduction of $\text{Fe}(\text{OH})^{2+}$ species to Fe^{2+} with $\bullet\text{OH}$ generation via reaction (4), as well as the photodecarboxylation of complexes of Fe(III) with generated carboxylic acids according to reaction (5).



This paper presents a comparative study on the degradation of *trans*-ferulic acid solutions at pH 3.0 by AO- H_2O_2 , EF and PEF using a stirred BDD/air-diffusion tank reactor. The mineralization process was also assessed by SPEF in order to check its potentiality at industrial scale. The effect of j and substrate concentration on the performance of the EAOPs tested was examined to understand the role of the generated hydroxyl radicals and the action of UV light. The decay of *trans*-ferulic acid and the evolution of some products like vanillin and carboxylic acids were monitored by high-performance liquid chromatography (HPLC). Primary aromatic intermediates were identified by gas chromatography-mass spectrometry (GC-MS). Based on the results obtained, a plausible route for *trans*-ferulic acid mineralization by EAOPs is proposed.

2. Experimental

2.1. Chemicals

trans-Ferulic acid (99% purity) and vanillin (99% purity) were supplied by Sigma-Aldrich and used without further purification. Fumaric, acetic and oxalic acids were of analytical grade supplied by Merck. Heptahydrated Fe(II) sulfate and anhydrous sodium sulfate were of analytical grade supplied by Fluka. Analytical grade sulfuric acid purchased from Merck was used to adjust the initial solution pH to 3.0. All the solutions were prepared with high-purity water from a Millipore

Milli-Q system (resistivity > 18 M Ω cm at 25 °C). Other chemicals used for analysis were of HPLC or analytical grade provided by Avocado, Fluka and Merck.

2.2. Electrolytic systems

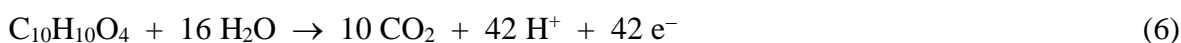
All the experiments were performed with an open, undivided, two-electrode cylindrical glass cell of 150 mL capacity. It was equipped with a double jacket for recirculating water at 35 °C by means of a Thermo Electron Corporation HAAKE DC 10 thermostat. This working temperature was chosen because it is the maximum value that can be used without significant water evaporation from the solution. All the assays were made under vigorous stirring with a magnetic bar at 700 rpm to ensure the transport of reactants toward/from the electrodes and homogenization. The electrodes were a BDD (deposited onto *p*-Si) anode purchased from NeoCoat (La-Chaux-de-Fonds, Switzerland) and a carbon-PTFE air-diffusion cathode purchased from E-TEK (Somerset, NJ, USA), both of 3 cm² geometric area and separated about 1 cm. The cathode was mounted as reported elsewhere [41] and was fed with air pumped at 300 mL min⁻¹ for H₂O₂ generation from reaction (2). The trials were carried out at constant *j* provided by an EG&G Princeton Applied Research 273A potentiostat-galvanostat.

Solutions of 100 mL containing *trans*-ferulic acid and 0.05 M Na₂SO₄ as background electrolyte at pH 3.0 were comparatively treated by AO-H₂O₂, EF and PEF. In the two latter EAOPs, 0.50 mM Fe²⁺ was added as catalyst since this content has been found optimal for many organics degraded under similar conditions [37-40]. For PEF, a Philips TL/6W/08 fluorescent black light blue tube of λ_{\max} = 360 nm with average power density of 5 W m⁻², determined with a Kipp&Zonen CUV 5 UV radiometer, was placed at 8 cm above the solution surface. Some experiments were also performed by SPEF upon direct exposition of the cell to sunlight irradiation in clear and sunny days of the summer 2015 in our laboratory of Barcelona (latitude: 41° 23'N, longitude: 2° 9'E). The average UV solar irradiation intensity from 300 to 400 nm was about 30 W m⁻², as measured on the radiometer. Before starting the experiments, the surfaces of the anode and

cathode were cleaned and activated, respectively, under polarization in 100 mL of a 0.05 M Na₂SO₄ solution at 100 mA cm⁻² for 180 min.

2.3. Apparatus and analytical methods

The solution pH was measured on a Crison GLP 22 pH-meter. For total organic carbon (TOC) measurements, samples were withdrawn from treated solutions, filtered with 0.45 μm PTFE filters purchased from Whatman and directly injected into a Shimadzu VCSN TOC analyzer, obtaining reproducible values with ±1% accuracy. From these data and considering that the total mineralization of *trans*-ferulic acid involves its conversion into CO₂ as follows:



the mineralization current efficiency (MCE) for each assay was estimated from Eq. (7) [37]:

$$\text{MCE (\%)} = \frac{n F V \Delta(\text{TOC})_{\text{exp}}}{4.32 \times 10^7 m I t} \times 100 \quad (7)$$

where n is the number of electrons related to the mineralization process (42 e⁻ according to reaction (6)), F is the Faraday constant (96487 C mol⁻¹), V is the solution volume (L), $\Delta(\text{TOC})_{\text{exp}}$ is the experimental TOC abatement (mg C L⁻¹), 4.32×10^7 is a conversion factor (3600 s h⁻¹ × 12000 mg C mol⁻¹), m is the number of carbon atoms of *trans*-ferulic acid (10 C atoms), I is the current (A) and t is the electrolysis time (h).

Treated solutions were analyzed by reversed-phase HPLC using a Waters 600 LC equipped with a BDS Hypersil C18 6 μm, 250 mm x 4.6 mm, column at 35 °C and coupled to a Waters 996 photodiode array detector. In the EF and PEF assays, the aqueous samples were diluted with acetonitrile to stop the degradation process and then filtered with 0.45 μm PTFE filters from Whatman. In all the measurements, 10 μL aliquots were injected into the LC and a 80% (v/v) acetonitrile/water mixture was eluted at 0.8 mL min⁻¹ as mobile phase. The chromatograms exhibited two well-defined peaks at retention time (t_r) of 3.37 min for *trans*-

ferulic acid and $t_r = 3.89$ min for vanillin, monitored at λ of 323 and 229 nm, respectively. Generated carboxylic acids were detected by ion-exclusion HPLC using the above LC fitted with a Bio-Rad Aminex HPX 87H, 300 mm \times 7.8 mm, column at 35 °C and the photodiode array detector selected at $\lambda = 210$ nm. Aliquots of 10 μ L were also injected into the LC and the mobile phase was 4 mM H₂SO₄ at 0.6 mL min⁻¹. The chromatograms displayed peaks related to oxalic ($t_r = 6.9$ min), acetic ($t_r = 14.9$ min) and fumaric ($t_r = 15.6$ min) acids.

The primary aromatic products of *trans*-ferulic acid were identified by electrolyzing 100 mL of a 0.834 mM substrate solution at 33.3 mA cm⁻² by AO-H₂O₂. Independent electrolyses were run up to 30 and 90 min and the organic components of the remaining solutions were extracted out with CH₂Cl₂ (3 \times 25 mL). Each organic fraction was dried over anhydrous Na₂SO₄, filtered and its volume reduced to about 1 mL to be further analyzed by GC-MS using a NIST05-MS library to interpret the mass spectra. GC-MS analysis was performed by coupling a 6890N GC and a 5975C MS from Agilent Technologies, operating in EI mode at 70 eV. The GC was fitted with either a non-polar Agilent J&W HP-5ms or a polar HP INNOWax column, both of 0.25 μ m, 30 m \times 0.25 mm. The temperature ramp was: 36 °C for 1 min, 5 °C min⁻¹ up to 300 °C or 250 °C for the non-polar or polar column, respectively, and hold time 10 min. The temperature of the inlet, source and transfer line was 250, 230 and 280 °C for the non-polar column and 250, 230 and 250 °C for the polar one.

3. Results and discussion

3.1. Decay of *trans*-ferulic acid by AO-H₂O₂, EF and PEF

A first series of trials was made by treating 100 mL of 0.834 mM *trans*-ferulic acid solutions in 0.05 M Na₂SO₄ at pH 3.0 by the different EAOPs to determine the decay kinetics of the substrate by reversed-phase HPLC. As a preliminary study, it was found that the substrate concentration of such solutions remained unchanged under a 6 W UVA irradiation in the absence of applied current, as

expected if this compound is not directly photolyzed by UVA radiation (data not shown). For the experiments using AO-H₂O₂ without catalyst, as well as for EF and PEF with 0.50 mM Fe²⁺, the solution pH dropped slightly from 3.0 to a final value near 2.7-2.8 after 360 min electrolysis, probably due to the generation of acidic products like final carboxylic acids [37-40].

Fig. 1a depicts a very slow decay of *trans*-ferulic acid by AO-H₂O₂, attaining 95% removal in 360 min. This means that this compound reacts very slowly with generated ROS, preferentially with BDD(•OH) originated from reaction (1). In contrast, Fig. 1b highlights a much faster abatement of *trans*-ferulic acid by EF and PEF, disappearing in about 15 and 10 min, respectively. The large acceleration can be ascribed to its very fast reaction in the bulk with •OH formed from Fenton's reaction (3) compared with the confined reaction taking place with BDD(•OH) near the anode. The slight increase in decay rate for PEF compared to EF suggests a very small participation of the photolytic reaction (4) to induce the production of higher amounts of •OH in the bulk.

The inset panels of Figs. 1a and b show the good linear fittings obtained for a pseudo-first-order kinetic analysis of the above concentration decays. This behavior suggests the generation of a steady concentration of BDD(•OH) and/or •OH during all treatments. Table 1 collects the apparent rate constants (k_1) and their excellent square regression coefficients (R^2) found for these assays. As can be seen, the k_1 value is quite similar in EF and PEF and approximately 3 orders of magnitude higher than that in AO-H₂O₂, confirming that in the two former EAOPs, *trans*-ferulic acid is slowly oxidized by BDD(•OH) and much more quickly by •OH in the bulk.

The kinetic study of the *trans*-ferulic acid decay was extended to lower concentrations of 0.167 and 0.417 mM operating at 33.3 mA cm⁻². Shorter time was needed for total removal of the substrate as the organic load decreased. For the PEF process, for example, the *trans*-ferulic acid disappeared at 10 min for 0.834 mM, but after only 7 min for 0.167 mM. According to this tendency, the good pseudo-first-order kinetics obtained for all the EAOPs showed an increasing k_1 value, as can be seen in Table 1. This behavior clearly indicates that the kinetic decay does not

actually obey a true pseudo-first-order reaction, since the same k_1 value should be determined regardless of the substrate content. Since quite similar amounts of BDD(\bullet OH) and/or \bullet OH are generated in each EAOP at 33.3 mA cm^{-2} when the organic matter content rises, a larger proportion of radicals is expected to react with the oxidation products formed and hence, a smaller quantity of them reacts with *trans*-ferulic acid, thus decelerating its abatement as experimentally found.

3.2. Mineralization of *trans*-ferulic acid solutions by AO-H₂O₂, EF and PEF

The mineralization of 0.834 mM *trans*-ferulic acid solutions at pH 3.0 was comparatively assessed for AO-H₂O₂, EF and PEF at $j = 33.3 \text{ mA cm}^{-2}$ by monitoring their TOC abatement. Fig. 2a shows a small but continuous mineralization under AO-H₂O₂ conditions, only achieving 72% TOC removal after 360 min of electrolysis. A much quicker TOC decay can be observed for EF, where TOC was finally reduced by 80%. Note that the mineralization process was very fast up to 90 min of EF because of the efficient action of \bullet OH, whereas it was progressively decelerated at longer time suggesting the formation of more recalcitrant products, like Fe(III)-carboxylate complexes, which are refractory to \bullet OH and slowly attacked by BDD(\bullet OH) [14]. In contrast, Fig. 2a evidences a very positive effect of UVA light in the PEF process since it is able to remove 95% TOC in 180 min, therefore attaining an almost total mineralization with 98% TOC reduction at 360 min. This large enhancement can be related to the photolysis of intermediates involving, for example, the photodecomposition of Fe(III)-carboxylate species via reaction (5) [14-16]. These results clearly indicate that the oxidation ability of the EAOPs grows in the sequence $\text{AO-H}_2\text{O}_2 \leq \text{EF} < \text{PEF}$.

Fig. 2b depicts the MCE values calculated from Eq. (7) for the trends given in Fig. 2a. As expected, the current efficiency rose as more oxidizing EAOPs were tested, although this behavior was more apparent at short electrolysis time, because the mineralization rate was particularly influenced by the oxidation with \bullet OH and the photolytic action of UVA light. In EF and, especially, the powerful PEF, the MCE values decayed dramatically from 43% and 81% at the beginning of the treatments to 13% and 15% at 360 min, respectively. This fall of current efficiency can be

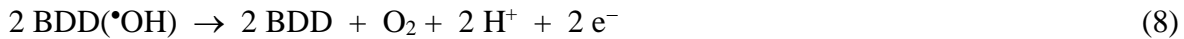
associated not only with the generation of more recalcitrant oxidation products but also with the gradual disappearance of organic matter [12,39,40]. In contrast, the current efficiency acquired a practically constant value of 11%-12% during the AO-H₂O₂ run, suggesting a steady mineralization rate of intermediates upon oxidation by BDD(•OH) alone.

Since j determines the amount of hydroxyl radicals produced in the EAOPs, the effect of this parameter between 16.7 and 100 mA cm⁻² on the mineralization of 0.834 mM *trans*-ferulic acid solutions was investigated. Table 1 collects the percentage of TOC removed after 360 min of all these treatments. For AO-H₂O₂ and EF, the mineralization degree underwent a progressive rise when j increased, as a result of the gradually greater production of oxidizing hydroxyl radicals. This means that the concomitant increase in rate of reaction (1) yields higher quantities of BDD(•OH) in AO-H₂O₂ while the enhancement of reaction (2) favors the larger accumulation of H₂O₂ that consequently accelerates the •OH formation from Fenton's reaction (3) in EF. Note that EF was more powerful than AO-H₂O₂ only up to 33.3 mA cm⁻², with higher j values leading to a similar final TOC removal in both cases. This suggests the formation of final products in EF, probably complexes with Fe(III), that are difficultly destroyed by BDD(•OH) and/or •OH, whereas the final species formed in AO-H₂O₂ can be more easily removed by increasing amounts of BDD(•OH). In PEF, Fig. 3a highlights a short activation time at the beginning of the electrolysis at 16.7 mA cm⁻², followed by a quick TOC decay to reach 96% reduction at 180 min, whereby the mineralization was strongly inhibited to be reduced by 98% at 360 min. However, a similar but faster TOC decay can be observed for greater j values, achieving up to 95-97% TOC reduction in 180 min. This is indicative of a very quick photolytic destruction of intermediates that are very slowly destroyed by BDD(•OH) and/or •OH. UVA irradiation is then so potent that, at 33.3 mA cm⁻², sufficient amounts of hydroxyl radicals are produced to yield products that can be completely photolyzed.

The current efficiency for each EAOP always decreased when j increased. This tendency can be easily deduced from the MCE values corresponding to the end of all trials, as listed in the last

column of Table 1. Fig. 3b exemplifies the MCE-time plots obtained for the powerful PEF process, showing the concomitant drop of current efficiency for all j values. The anomalous behavior observed in this figure up to 60-90 min at 16.7 mA cm^{-2} is due to the induction period required under such a low j value, probably because the poor production of hydroxyl radicals entails a slower appearance of intermediates that can be rapidly photolyzed by UVA light.

The decay in MCE at higher j is contrary to the quicker TOC removal found. This behavior is typical of EAOPs and can be ascribed to the destruction of the excess of generated hydroxyl radicals by non-oxidizing wasting reactions. They include the anodic oxidation of physisorbed BDD($\bullet\text{OH}$) radicals to O_2 by reaction (8) and the destruction of $\bullet\text{OH}$ by H_2O_2 and Fe^{2+} from reactions (9) and (10), respectively, along with the larger enhancement of the anodic formation of other weaker oxidants such as ozone by reaction (11) and $\text{S}_2\text{O}_8^{2-}$ ion from SO_4^{2-} ion by reaction (12), thus inhibiting the H_2O discharge from reaction (1) [12-16].



The influence of the substrate concentration in the range $0.167 - 1.668 \text{ mM}$ on the mineralization of *trans*-ferulic solutions upon application of the EAOPs was examined at the best j of 33.3 mA cm^{-2} found for PEF. A look at Table 1 reveals that TOC removals of 67%-74% and slightly higher values of 74%-80% were achieved in AO- H_2O_2 and EF, respectively. In fact, AO- H_2O_2 showed lower oxidation ability than EF up to 0.843 mM , whereas both methods had a similar mineralization power for higher substrate concentrations. Despite the similar mineralization attained

in each of these EAOPs regardless of the *trans*-ferulic content, a careful inspection of Table 1 indicates a progressive increase of the corresponding final current efficiency when raising the initial substrate amount. For AO-H₂O₂, for example, the MCE grew from 2.3% at 0.164 mM to 21% at 1.668 mM. As mentioned above, similar quantities of hydroxyl radicals are expected to be generated in each EAOP at a given *j* and thus, one can infer that a larger organic matter content favors the reaction of BDD(•OH) and/or •OH with oxidation products, thereby decelerating their wasting reactions (8)-(12). This also takes place for the PEF process, as can be deduced from the data of Table 1. Fig. 4a depicts the very high oxidation power of this method, which was even able to yield a 98% mineralization for the most concentrated 1.668 mM solution due to the additional quick photodecomposition of intermediates under UVA irradiation. The corresponding MCE-time plots of Fig. 4b highlight again the drop of the current efficiency at prolonged electrolysis because of the gradual generation of highly recalcitrant products and the loss of organic matter, as stated above. The MCE value increased with increasing substrate content as well, due to the larger oxidation with hydroxyl radicals to generate more products that can be rapidly photolyzed. At the end of these PEF treatments, the current efficiency varied from 2.9% for 0.164 mM to a high value of 31% for 1.668 mM. All these findings allow concluding that the treatment of more concentrated solutions largely upgrades the mineralization process of *trans*-ferulic acid solutions.

3.3. SPEF treatment of *trans*-ferulic acid solutions

In view of the excellent results found for the PEF process, some experiments were made by degrading *trans*-ferulic acid solutions by SPEF at several *j* values for 180 min. Fig. 5a presents the quick TOC abatement found in these trials, which was even much faster than that obtained by PEF under comparable conditions (see Figs. 3a and 4a) because of the higher UV intensity supplied by sunlight. As can be observed, a 0.834 mM substrate solution at 33.3 mA cm⁻² reached 93% mineralization in 120 min, without further TOC removal at longer time. At 100 mA cm⁻², the higher production of hydroxyl radicals along with the quicker photolysis of oxidation products allowed

attaining equal final TOC decay in only about 60 min. At that time, a 0.417 mM solution treated at 33.3 mA cm⁻² already reached a steady mineralization with near 84% TOC reduction. The fact that SPEF yielded a smaller final mineralization degree than PEF at the same j values (see Fig. 5a and Table 1) indicates that the quicker photolysis of some intermediates by the more potent sunlight led to a larger accumulation of highly recalcitrant products.

Fig. 5b depicts that the MCE values for the SPEF trials of Fig. 5a showed the same trends already discussed for the other EAOPs, such as a gradual drop of current efficiency (i) at longer electrolysis, (ii) when the initial substrate concentration becomes too low and by (iii) at higher j , owing to the reasons pointed out above. For the best SPEF treatment of a 0.834 mM *trans*-ferulic acid solution at 33.3 mA cm⁻², a 44% MCE was found at 120 min when the maximum 93% TOC removal was reached.

The aforementioned findings corroborate the viability of SPEF for the remediation of wastewater containing *trans*-ferulic acid at industrial level. The method becomes more efficient using concentrated solutions and operating at a low j such as 33.3 mA cm⁻².

3.4. Identification and evolution of aromatic products and generated carboxylic acids

Table 2 summarizes the characteristics of the four primary aromatic products of *trans*-ferulic acid (**1**) detected by GC-MS at 30 and 90 min of electrolysis of a 0.834 mM solution of pH 3.0 by AO-H₂O₂ at 33.3 mA cm⁻². Compound **2** arises from the decarboxylation of **1**, whereas compounds **3-5** are produced by its further oxidation. It is noticeable that the generation of compound **5** (vanillin) has also been reported during the degradation of *trans*-ferulic acid by •OH radicals originated in TiO₂ photocatalysis [11].

On the basis of the above GC-MS results, the change of the concentration of compound **5** during the degradation of 0.834 mM *trans*-ferulic acid solutions at 33.3 mA cm⁻² under the conditions of Fig. 1 was followed from its characteristic peak recorded by reversed-phase HPLC. Only traces of this product (< 0.005 mM) were found under AO-H₂O₂ treatment, suggesting that it

was destroyed by BDD(\bullet OH) and produced from the oxidation of **1** at a similar rate. This hypothesis was confirmed from the rapid accumulation and disappearance of **5** under EF and PEF conditions, as shown in Fig. 6a. A similar content of this product can be observed during both treatments, with a maximum value of 0.0030 mM at ca. 6 min and almost total removal at 15 min, i.e., when the parent molecule **1** had been just removed (see Fig. 1b). These results point to a very quick reaction of **1** and its primary aromatic products with \bullet OH in the bulk, whereas the subsequent products are much more slowly destroyed by hydroxyl radicals, therefore decelerating the mineralization process (see Fig. 2a)

It is well known that the cleavage of the benzene ring of aromatic compounds originates linear products that evolve to short aliphatic carboxylic acids [13-17]. To explore this possibility for *trans*-ferulic acid mineralization, the solutions treated under the conditions of Fig. 2 were analyzed by ion-exclusion HPLC. Final carboxylic acids such as fumaric (**6**), acetic (**7**) and oxalic (**8**) were detected and quantified by this technique. While the two former acids are oxidized to the latter one, acid **8** can be directly converted into CO₂ [14,16]. In the EF and PEF treatments, all these acids tend to form Fe(III) complexes, which are slowly oxidized by BDD(\bullet OH) and more difficultly attacked by \bullet OH in the bulk [37-40].

Low contents of acids **6** and **7** (< 0.017 mM) appeared up to 30-60 min in all treatments, as expected from the fast removal of these compounds and their Fe(III) complexes. In contrast, the final acid **8** was much more largely accumulated in all cases evidencing that it was the main carboxylic acid produced in the mineralization process. Fig. 6b shows a progressive accumulation with slow drop of acid **8** up to a final value of 0.13 mM for AO-H₂O₂. This value accounts for 3.1 mg L⁻¹ of TOC, which constitutes 11% of the organic load of the remaining solution (see Table 1). For EF and PEF, Fig. 6b reveals that the much quicker destruction of primary intermediates by \bullet OH led to about 0.76-0.78 mM of acid **8** as maximal at 60-90 min, its further fall depending on the applied treatment. In EF, the slow oxidation of Fe(III)-oxalate complexes by BDD(\bullet OH) yielded

0.39 mM of final acid **8**, corresponding to 9.4 mg L⁻¹ of TOC and a 47% of the organic load of the final solution (see Table 1). This means that the final solution of EF still contained 53% of undetected products that are highly recalcitrant to hydroxyl radicals. On the other hand, the UVA light in PEF caused the quick and overall photodecarboxylation of Fe(III)-oxalate complexes via reaction (5), as highlighted in Fig. 6b, although a 2% of the starting TOC remained in the final solution (see Table 1). Consequently, the PEF process allows the oxidation of most of undetected recalcitrant products that cannot be destroyed by hydroxyl radicals in EF, thanks to the photolytic action of UVA radiation. This behavior along with the total removal of final carboxylic acids explains the almost total mineralization of *trans*-ferulic acid solutions achieved using the powerful PEF process.

3.5. Plausible reaction pathway for *trans*-ferulic acid treated by EAOPs with BDD

On the basis of the products detected by GC-MS and HPLC, a plausible reaction pathway is proposed in Fig. 7 for *trans*-ferulic acid mineralization by EAOPs with BDD anode. Oxidation of aromatics takes place via reaction with BDD([•]OH) in AO-H₂O₂ and much more rapidly with [•]OH in EF, PEF and SPEF, whereas that of final carboxylic acids and Fe(III)-carboxylate species involves preferentially the attack of BDD([•]OH). A much slower degradation with other generated oxidants like H₂O₂, HO₂[•], O₃ and S₂O₈²⁻ may occur as well. Only the fate of Fe(III) complexes with oxalic acid, but not of the other carboxylic acids, is stated for sake of simplicity.

The process starts with the decarboxylation of **1** to yield **2**. Further oxidation of the side vinyl group of **2** yields **3** with a lateral ethyl group, which can then be oxidized either to the ketone **4** with demethylation or to the aldehyde **5**. Subsequent degradation of all these aromatics with cleavage of the benzene ring leads to a mixture of final acids **6-8**. Acids **6** and **7** are formed to a small extent and quickly converted into acid **8**. This acid is directly transformed into CO₂ by BDD([•]OH) in AO-H₂O₂, but, in EF, PEF and SPEF, it forms Fe(III)-oxalate species that are slowly mineralized by

BDD(\bullet OH) and much more rapidly photodecomposed under UVA light or sunlight, regenerating Fe^{2+} according to reaction (5).

4. Conclusions

The PEF treatment of *trans*-ferulic acid solutions of pH 3.0 is able to yield almost total mineralization with 98% TOC reduction for substrate contents ≥ 0.843 mM and $j \geq 16.7$ mA cm⁻². It is much powerful than EF, which allowed 92% TOC abatement as maximal at 100 mA cm⁻², because of the enhancement of the destruction of highly recalcitrant products to hydroxyl radicals by UVA irradiation. The oxidation ability of AO-H₂O₂ was slightly lower than that of EF up to 0.843 mM *trans*-ferulic acid and $j = 33.3$ mA cm⁻², both methods possessing similar mineralization power for higher substrate concentrations and j values. The decay of *trans*-ferulic acid concentration by AO-H₂O₂ was very slow by its poor reaction with BDD(\bullet OH), being much faster in EF and PEF due to its much quicker reaction with \bullet OH in the bulk. For each EAOP, increasing j from 16.7 to 100 mA cm⁻² caused faster mineralization with lower MCE, whereas the change of substrate concentration from 0.167 to 1.668 mM gave similar percentage of final TOC removed with a concomitant growth of current efficiency. The SPEF treatment accelerated the mineralization compared with PEF, although it also promoted the accumulation of a slightly larger proportion of barely oxidizable products. Four aromatic products and three short carboxylic acids were identified. Oxalic acid was the most important product and its total disappearance in PEF in contrast to its large persistence in AO-H₂O₂ and EF explained the superior oxidation power of the former EAOP.

Acknowledgments

The authors thank MINECO (Spain) for financial support under project CTQ2013-48897-C2-1-R, co-financed with FEDER funds. The Ph.D. fellowship awarded to N. Flores from SENESCYT (Ecuador) is also acknowledged.

References

- [1] U.T. Un, U. Altay, A.S. Koparal, U.B. Ogutveren, Complete treatment of olive mill wastewaters by electrooxidation, *Chem. Eng. J.* 139 (2008) 445-452.
- [2] S. Magdich, C. Ben Ahmed, R. Jarboui, B. Ben Rouina, M. Boukhris, E. Ammar, Dose and frequency dependent effects of olive mill wastewater treatment on the chemical and microbial properties of soil, *Chemosphere* 93 (2013) 1896-1903.
- [3] S. Dermeche, M. Nadour, C. Larroche, F. Moulti-Mati, P. Michaud, Olive mill wastes: Biochemical characterizations and valorization strategies, *Process Biochem.* 48 (2013) 1532-1552.
- [4] J.M. Ochando-Pulido, M.D. Victor-Ortega, G. Hodaifa, A. Martinez-Ferez, Physicochemical analysis and adequation of olive oil mill wastewater after advanced oxidation process for reclamation by pressure-driven membrane technology, *Sci. Total Environ.* 503-504 (2014) 113-121.
- [5] M. DellaGreca, L. Previtiera, F. Temussi, A. Zarrelli, Low-molecular-weight components of olive oil mill waste-waters, *Phytochem. Anal.* 15 (2004) 184-188.
- [6] C. Mancuso, R. Santangelo, Ferulic acid: Pharmacological and toxicological aspects, *Food Chem. Toxicol.* 65 (2014) 185-195.
- [7] N. Kumar, V. Pruthi, Potential applications of ferulic acid from natural sources, *Biotechnol. Reports* 4 (2014) 86-93.
- [8] M.A. Miranda, F. Galindo, A.M. Amat, A. Arques, Pyrilyum salt-photosensitized degradation of phenolic contaminants derived from cinnamic acid with solar light. Correlation of the observed reactivities with fluorescence quenching, *Appl. Catal. B: Environ.* 28 (2000) 127-133.

- [9] B.R. Yadav, A. Garg, Catalytic wet oxidation of ferulic acid (a lignin model compound) in the presence of non-noble metal based catalysts at mild conditions, *Chem. Eng. J.* 252 (2014) 185-193.
- [10] R. Andreozzi, M. Canterino, V. Caprio, I. Di Somma, R. Marotta, Use of an amorphous iron oxide hydrated as catalyst for hydrogen peroxide oxidation of ferulic acid in water, *J. Hazard. Mater.* 152 (2008) 870-875.
- [11] V. Augugliaro, G. Camera-Roda, V. Loddo, G. Palmisano, L. Palmisano, F. Parrino, Synthesis of vanillin in water by TiO₂ photocatalysis, *Appl. Catal. B: Environ.* 111-112 (2012) 555-561.
- [12] M. Panizza, G. Cerisola, Direct and mediated anodic oxidation of organic pollutants, *Chem. Rev.* 109 (2009) 6541-6569.
- [13] I. Sirés, E. Brillas, Remediation of water pollution caused by pharmaceutical residues based on electrochemical separation and degradation technologies: a review, *Environ. Int.* 40 (2012) 212-229.
- [14] I. Sirés, E. Brillas, M.A. Oturan, M.A. Rodrigo, M. Panizza, Electrochemical advanced oxidation processes: today and tomorrow. A review, *Environ. Sci. Pollut. Res.* 21 (2014) 8336-8367.
- [15] S. Vasudevan, M.A. Oturan, Electrochemistry: As cause and cure in water pollution-an overview, *Environ. Chem. Lett.* 12 (2014) 97-108.
- [16] E. Brillas, C.A. Martínez-Huitle, Decontamination of wastewaters containing synthetic organic dyes by electrochemical methods. An updated review, *Appl. Catal. B: Environ.* 166-167 (2015) 603-643.
- [17] B. Boye, P.A. Michaud, B. Marselli, M.M. Dieng, E. Brillas, C. Comninellis, Anodic oxidation of 4-chlorophenoxyacetic acid on synthetic boron-doped diamond electrodes, *New Diamond Front. Carbon Technol.* 12 (2002) 63-72.

- [18] B. Marselli, J. Garcia-Gomez, P.A. Michaud, M.A. Rodrigo, C. Comninellis, Electrogeneration of hydroxyl radicals on boron-doped diamond electrodes, *J. Electrochem. Soc.* 150 (2003) D79-D83.
- [19] C.A. Martínez-Huitle, S. Ferro, Electrochemical oxidation of organic pollutants for the wastewater treatment: direct and indirect processes, *Chem. Soc. Rev.* 35 (2006) 1324-1340.
- [20] M. Hamza, R. Abdelhedi, E. Brillas, I. Sirés, Comparative electrochemical degradation of the triphenylmethane dye Methyl Violet with boron-doped diamond and Pt anodes, *J. Electroanal. Chem.* 627 (2009) 41-50.
- [21] L. Ciríaco, C. Anjo, J. Correia, M.J. Pacheco, A. Lopes, Electrochemical degradation of ibuprofen on Ti/Pt/PbO₂ and Si/BDD electrodes, *Electrochim. Acta* 54 (2009) 1464-1472.
- [22] M.A. Rodrigo, P. Cañizares, A. Sánchez-Carretero, C. Sáez, Use of conductive-diamond electrochemical oxidation for wastewater treatment, *Catal. Today* 151 (2010) 173-177.
- [23] E.B. Cavalcanti, S. Garcia-Segura, F. Centellas, E. Brillas, Electrochemical incineration of omeprazole in neutral aqueous medium using a platinum or boron-doped diamond. Degradation kinetics and oxidation products, *Water Res.* 47 (2013) 1803-1815.
- [24] A. Wang, J. Qu, H. Liu, J. Ru, Mineralization of an azo dye Acid Red 14 by photoelectro-Fenton process using an activated carbon fiber cathode, *Appl. Catal. B: Environ.* 84 (2008) 393-399.
- [25] A. Khataee, A. Khataee, M. Fathinia, B. Vahid, S.W. Joo, Kinetic modeling of photoassisted-electrochemical process for degradation of an azo dye using boron-doped diamond anode and cathode with carbon nanotubes, *J. Ind. Eng. Chem.* 19 (2013) 1890-1894.
- [26] A. Khataee, A. Akbarpour, B. Vahi, Photoassisted electrochemical degradation of an azo dye using Ti/RuO₂ anode and carbon nanotubes containing gas-diffusion cathode, *J. Taiwan Inst. Chem. Eng.* 45 (2014) 930-936.

- [27] V. Vatanpour, N. Daneshvar, M.H. Rasoulifard, Electro-Fenton degradation of synthetic dye mixture: influence of intermediates, *J. Environ. Eng. Manage.* 19 (2009) 277-282.
- [28] M.H.M.T. Assumpção, A. Moraes, R.F.B. De Souza, R.M. Reis, R.S. Rocha, I. Gaubeur, M.L. Calegari, P. Hammer, M.R.V. Lanza, M.C. Santos, Degradation of dipyrone via advanced oxidation processes using a cerium nanostructured electrocatalyst material, *Appl. Catal. A: Gen.* 462-463 (2013) 256-261.
- [29] A. Dirany, I. Sirés, N. Oturan, A. Özcan, M.A. Oturan, Electrochemical treatment of the antibiotic sulfachloropyridazine: kinetics, reaction pathways, and toxicity evolution. *Environ. Sci. Technol.* 46 (2012) 4074-4082.
- [30] M.S. Yahya, N. Oturan, K. El Kacemi, M. El Karbane, C.T. Aravindakumar, M.A. Oturan, Oxidative degradation study on antimicrobial agent ciprofloxacin by electro-Fenton process: Kinetics and oxidation products, *Chemosphere* 117 (2014) 447-454.
- [31] A. El-Ghenemy, R.M. Rodríguez, E. Brillas, N. Oturan, M.A. Oturan, Electro-Fenton degradation of the antibiotic sulfanilamide with Pt/carbon-felt and BDD/carbon-felt cells. Kinetics, reaction intermediates, and toxicity assessment, *Environ. Sci. Pollut. Res.* 21 (2014) 8368-8378.
- [32] S. Ammar, R. Abdelhedi, C. Flox, C. Arias, E. Brillas, Electrochemical degradation of the dye indigo carmine at boron-doped diamond anode for wastewaters remediation, *Environ. Chem. Lett.* 4 (2006) 229-233.
- [33] A. Thiam, M. Zhou, E. Brillas, I. Sirés, Two-step mineralization of Tartrazine solutions: Study of parameters and by-products during the coupling of electrocoagulation with electrochemical advanced oxidation processes, *Appl. Catal. B: Environ.* 150-151 (2014) 116-125.

- [34] A. Thiam, I. Sirés, J.A. Garrido, R.M. Rodríguez, E. Brillas, Decolorization and mineralization of Allura Red AC aqueous solutions by electrochemical advanced oxidation processes, *J. Hazard. Mater.* 290 (2015) 34-42.
- [35] K. Cruz-González, O. Torres-López, A. García-León, J.L. Guzmán-Mar, L.H. Reyes, A. Hernández-Ramírez, J.M. Peralta-Hernández, Determination of optimum operating parameters for Acid Yellow 36 decolorization by electro-Fenton process using BDD cathode, *Chem. Eng. J.* 160 (2010) 199-206.
- [36] K. Cruz-González, O. Torres-López, A. García-León, E. Brillas, A. Hernández-Ramírez, J.M. Peralta-Hernández, Optimization of electro-Fenton/BDD process for decolorization of a model azo dye wastewater by means of response surface methodology, *Desalination* 286 (2012) 63-68.
- [37] E.J. Ruiz, A. Hernández-Ramírez, J.M. Peralta-Hernández, C. Arias, E. Brillas, Application of solar photoelectro-Fenton technology to azo dyes mineralization: Effect of current density, Fe^{2+} and dye concentrations, *Chem. Eng. J.* 171 (2011) 385-392.
- [38] F.C. Moreira, S. Garcia-Segura, V.J.P. Vilar, R.A.R. Boaventura, E. Brillas, Decolorization and mineralization of Sunset Yellow FCF azo dye by anodic oxidation, electro-Fenton, UVA photoelectro-Fenton and solar photoelectro-Fenton processes, *Appl. Catal. B: Environ.* 142-143 (2013) 877-890.
- [39] X. Florenza, A.M.S. Solano, F. Centellas, C.A. Martínez-Huitle, E. Brillas, S. Garcia-Segura, Degradation of the azo dye Acid Red 1 by anodic oxidation and indirect electrochemical processes based on Fenton's reaction chemistry. Relationship between decolorization, mineralization and products, *Electrochim. Acta* 142 (2014) 276-288.
- [40] A. Thiam, I. Sirés, F. Centellas, P.L. Cabot, E. Brillas, Decolorization and mineralization of Allura Red AC azo dye by solar photoelectro-Fenton: Identification of intermediates, *Chemosphere* 136 (2015) 1-8.

- [41] B. Boye, M.M. Dieng, E. Brillas, Electrochemical degradation of 2,4,5-trichlorophenoxyacetic acid in aqueous medium by peroxi-coagulation. Effect of pH and UV light, *Electrochim. Acta* 48 (2003) 781-790.

Figure captions

Fig. 1. Variation of *trans*-ferulic acid concentration with electrolysis time for the degradation of 100 mL of a 0.834 mM substrate solution in 0.05 M Na₂SO₄ at pH 3.0 and 35 °C using a BDD/air-diffusion cell of 3 cm² electrode area by applying 33.3 mA cm⁻². In (a), anodic oxidation with electrogenerated H₂O₂ (AO-H₂O₂). In (b), (△) electro-Fenton (EF) with addition of 0.50 mM Fe²⁺ and (▲) photoelectro-Fenton (PEF) with addition of 0.50 mM Fe²⁺ using a 6 W UVA light. The inset panels depict the pseudo-first-order kinetics found for the *trans*-ferulic acid content abatement.

Fig. 2. Change of (a) TOC and (b) mineralization current efficiency with electrolysis time under the same conditions of Fig. 1. Method: (○) AO-H₂O₂, (△) EF and (▲) PEF.

Fig. 3. Influence of current density on (a) TOC decay and (b) mineralization current efficiency vs. electrolysis time for the PEF treatment of 100 mL of a 0.834 mM *trans*-ferulic acid solution in 0.05 M Na₂SO₄ with 0.50 mM Fe²⁺ at pH 3.0 and 35 °C using a BDD/air-diffusion cell. Applied current density: (●) 16.7 mA cm⁻², (▲) 33.3 mA cm⁻², (◆) 66.7 mA cm⁻² and (▼) 100 mA cm⁻².

Fig. 4. Effect of *trans*-ferulic acid concentration on (a) TOC removal and (b) mineralization current efficiency vs. electrolysis time for the PEF degradation of 100 mL of solutions of this substrate in 0.05 M Na₂SO₄ with 0.50 mM Fe²⁺ at pH 3.0 using a BDD/air-diffusion cell at 33.3 mA cm⁻² and 35 °C. Content of *trans*-ferulic acid: (●) 0.167 mM, (◆) 0.417 mM, (▲) 0.834 mM and (■) 1.668 mM.

Fig. 5. Variation of: (a) TOC and (b) mineralization current efficiency with electrolysis time for the solar PEF (SPEF) degradation of 100 mL of *trans*-ferulic acid solutions in 0.05 M Na₂SO₄ with 0.50 mM Fe²⁺ at pH 3.0 and 35 °C using a BDD/air-diffusion cell. Content of *trans*-ferulic acid: (■,▼) 0.834 mM and (◆) 0.417 mM. Current density: (■,◆) 33.3 mA cm⁻² and (▼) 100 mA cm⁻².

Fig. 6. Time-course of the concentration of (a) vanillin (**5**) and (b) oxalic acid (**8**) detected during the treatments shown in Fig. 1. Method: (○) AO-H₂O₂, (△) EF and (▲) PEF.

Fig. 7. Reaction pathway proposed for *trans*-ferulic acid mineralization by AO-H₂O₂, EF, PEF and SPEF using a BDD/air-diffusion cell. The species •OH in the sequence of aromatics accounts for by their oxidation by BDD(•OH) at the BDD surface and/or •OH from Fenton's reaction in the bulk.

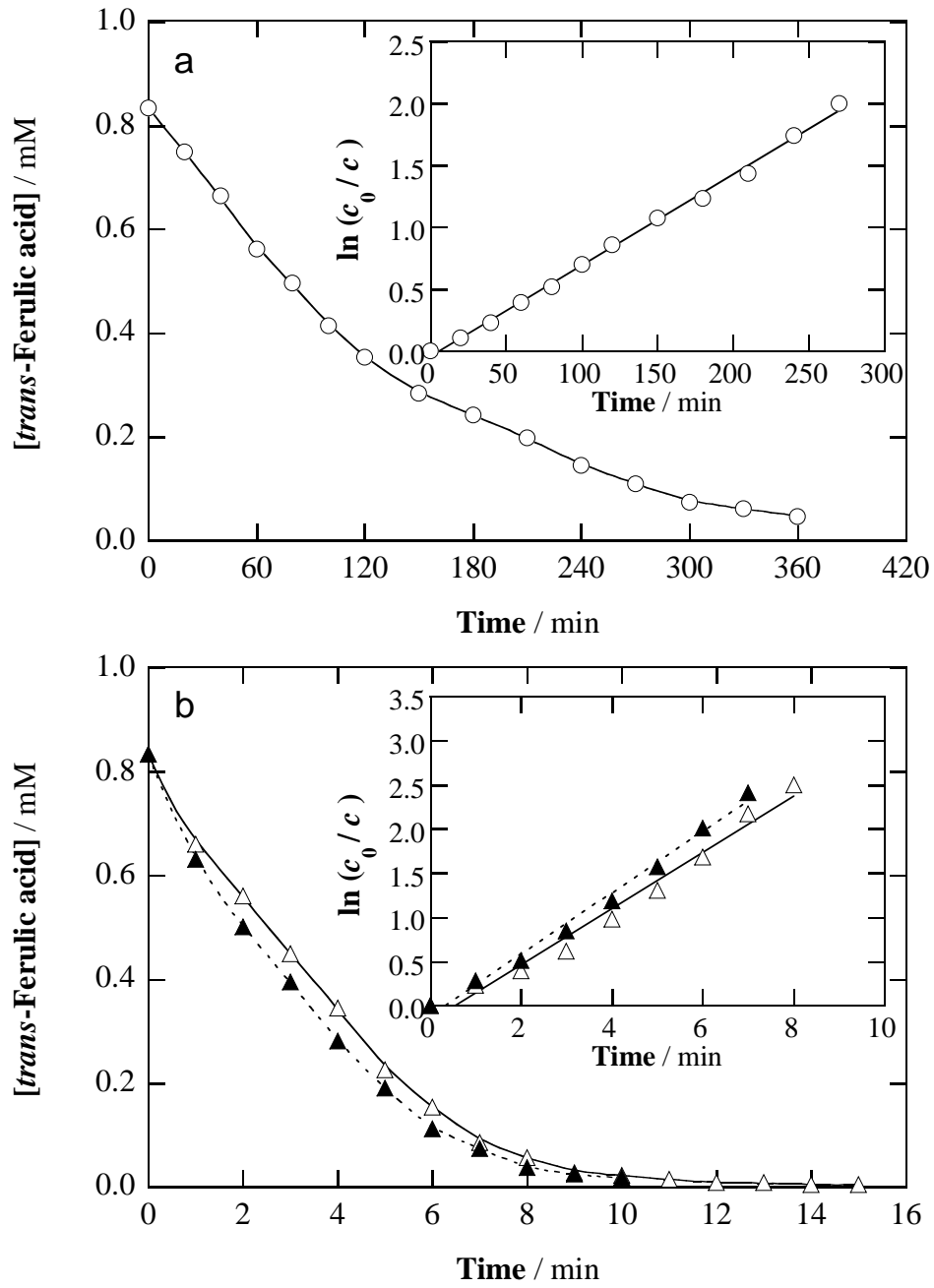


Fig. 1

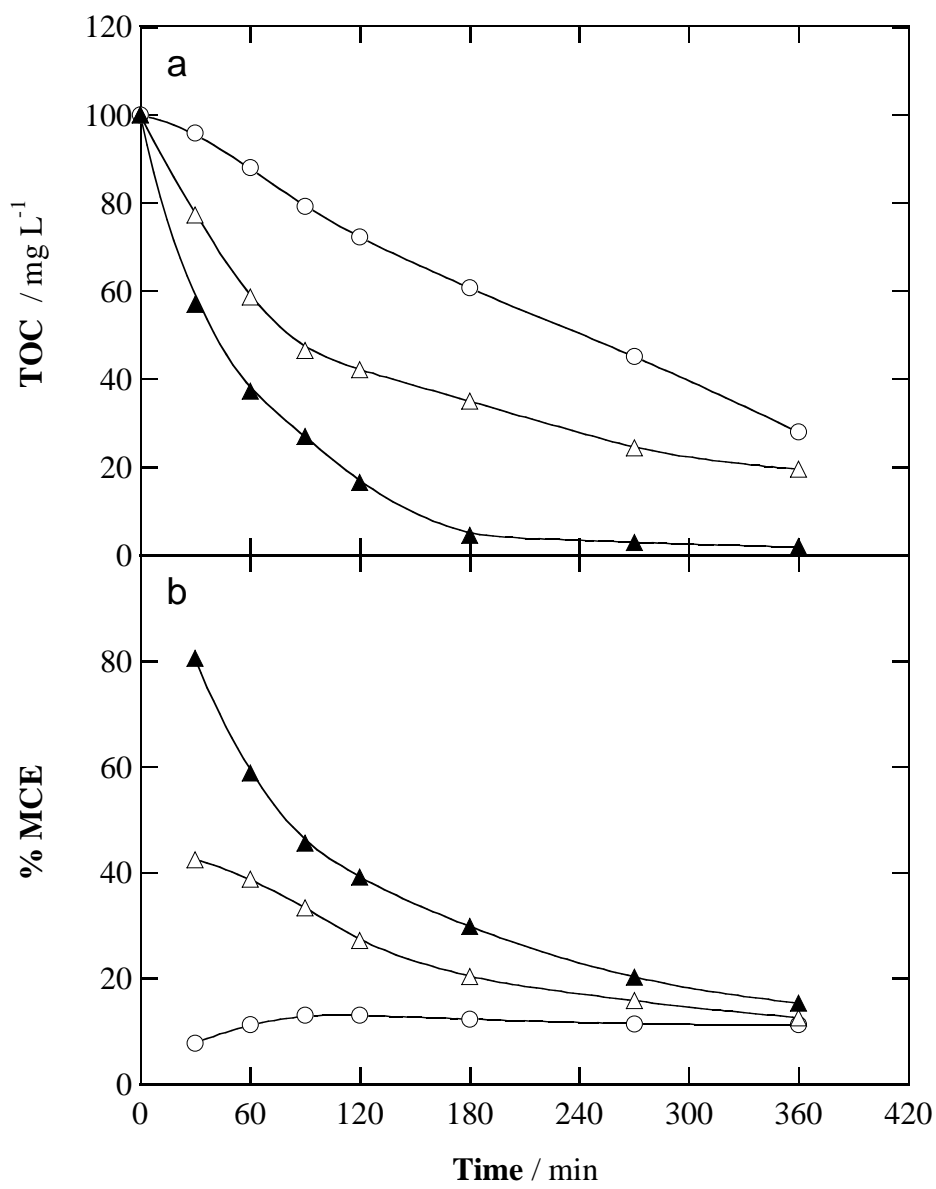


Fig. 2

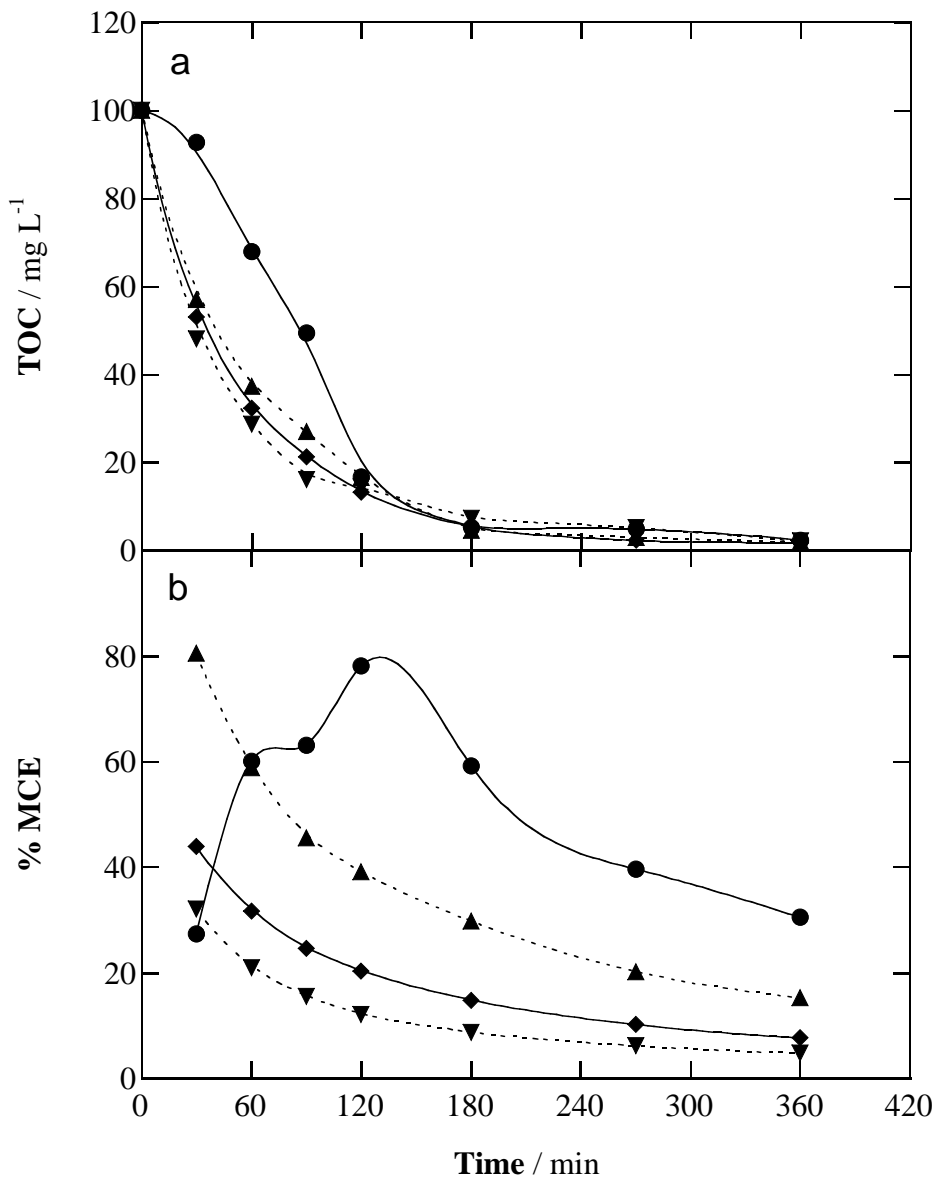


Fig. 3

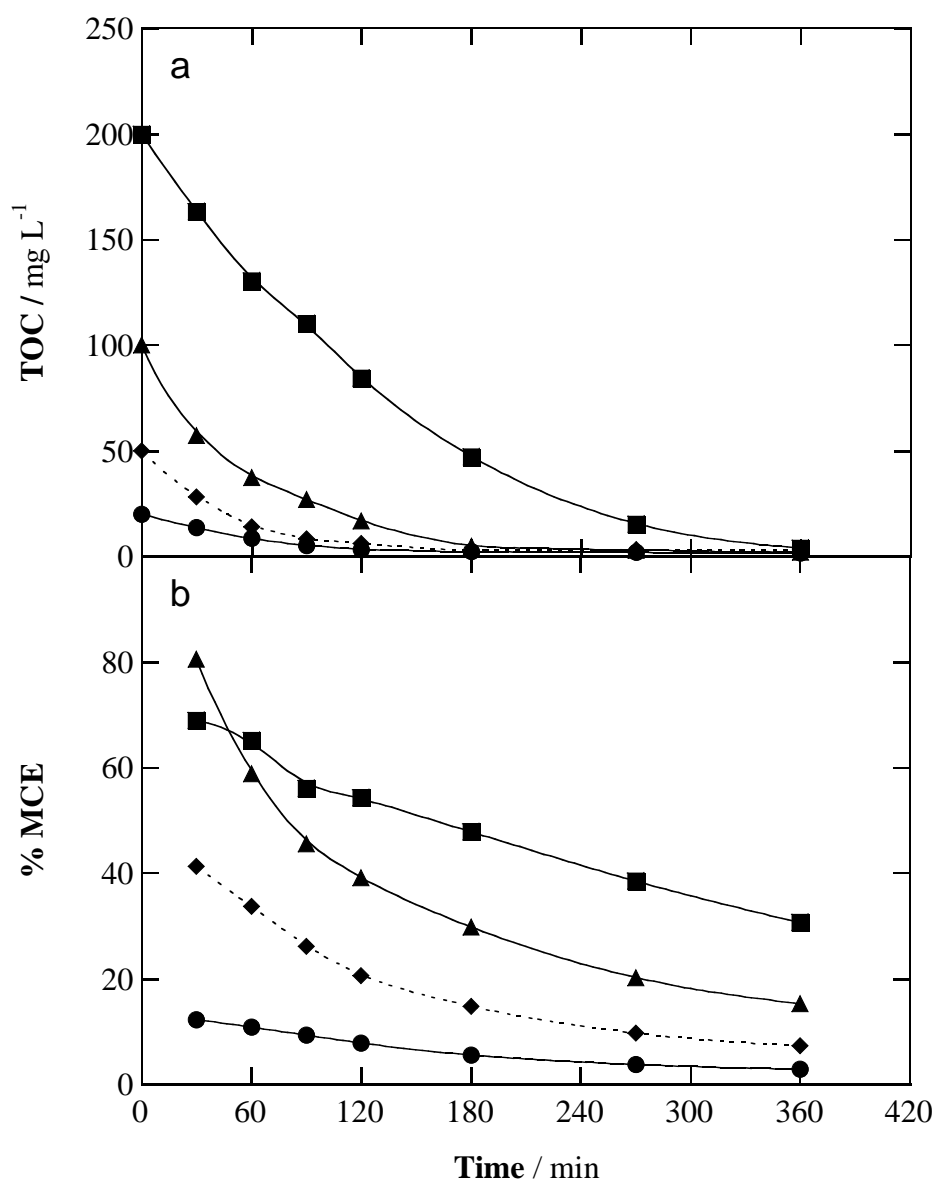


Fig. 4

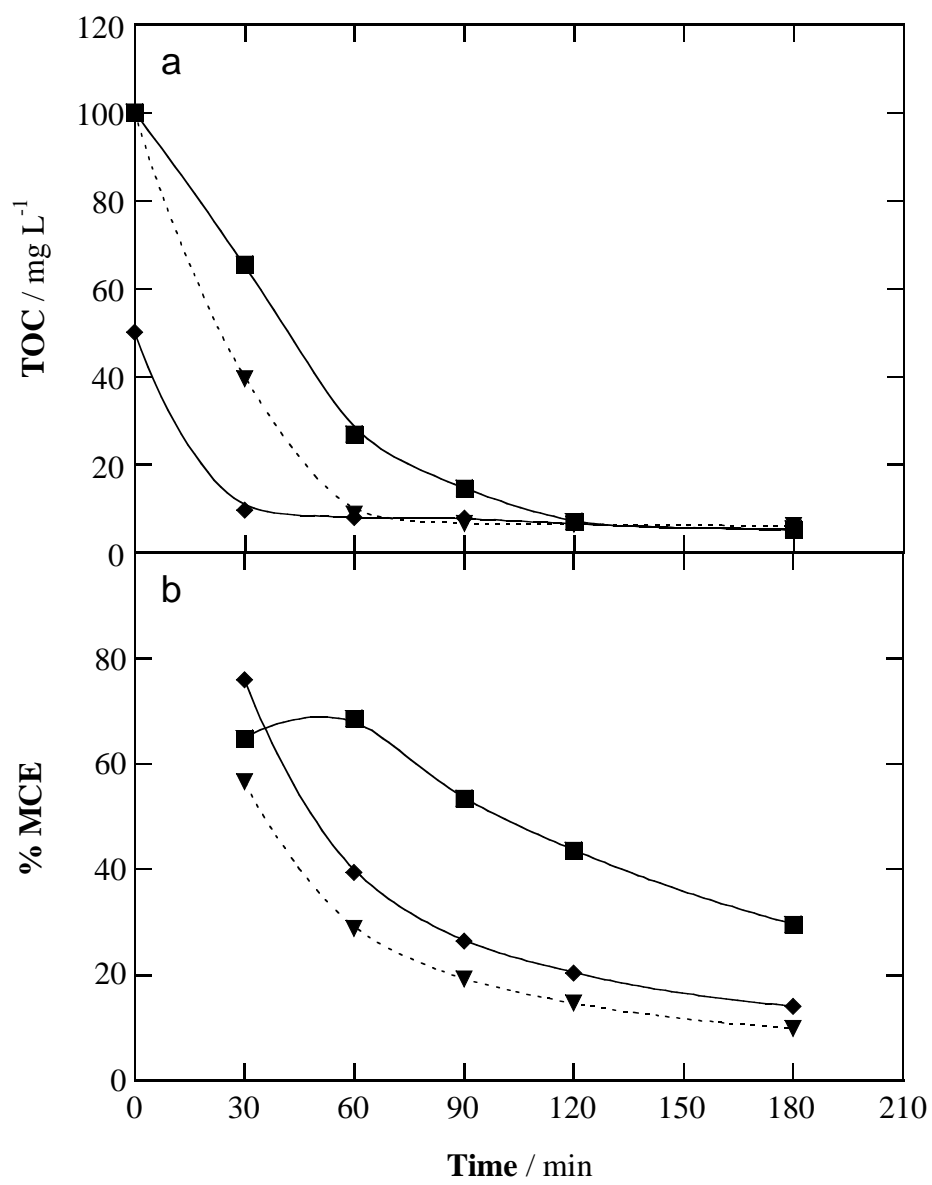


Fig. 5

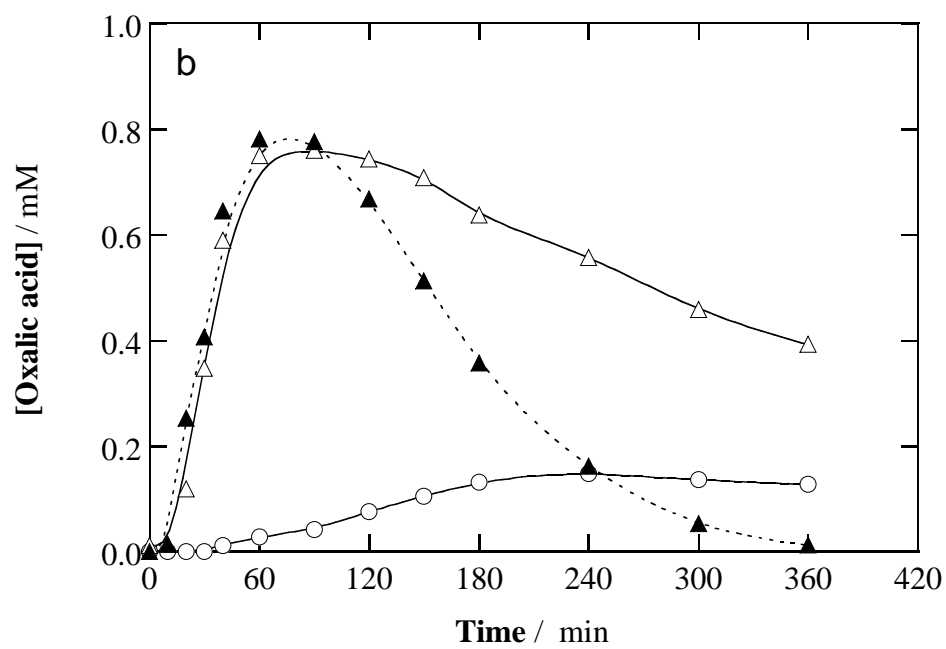
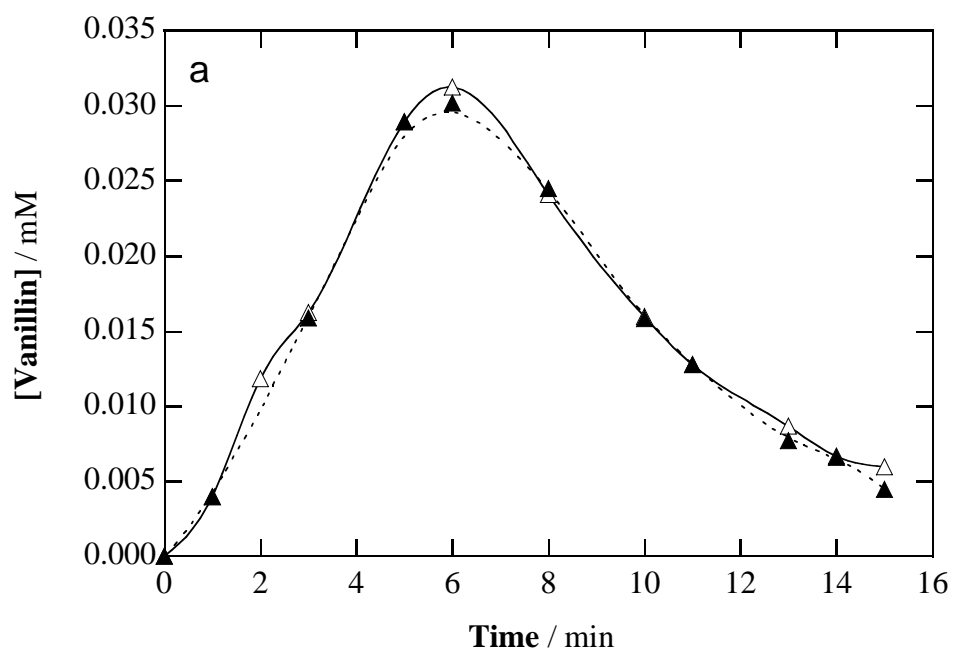


Fig. 6

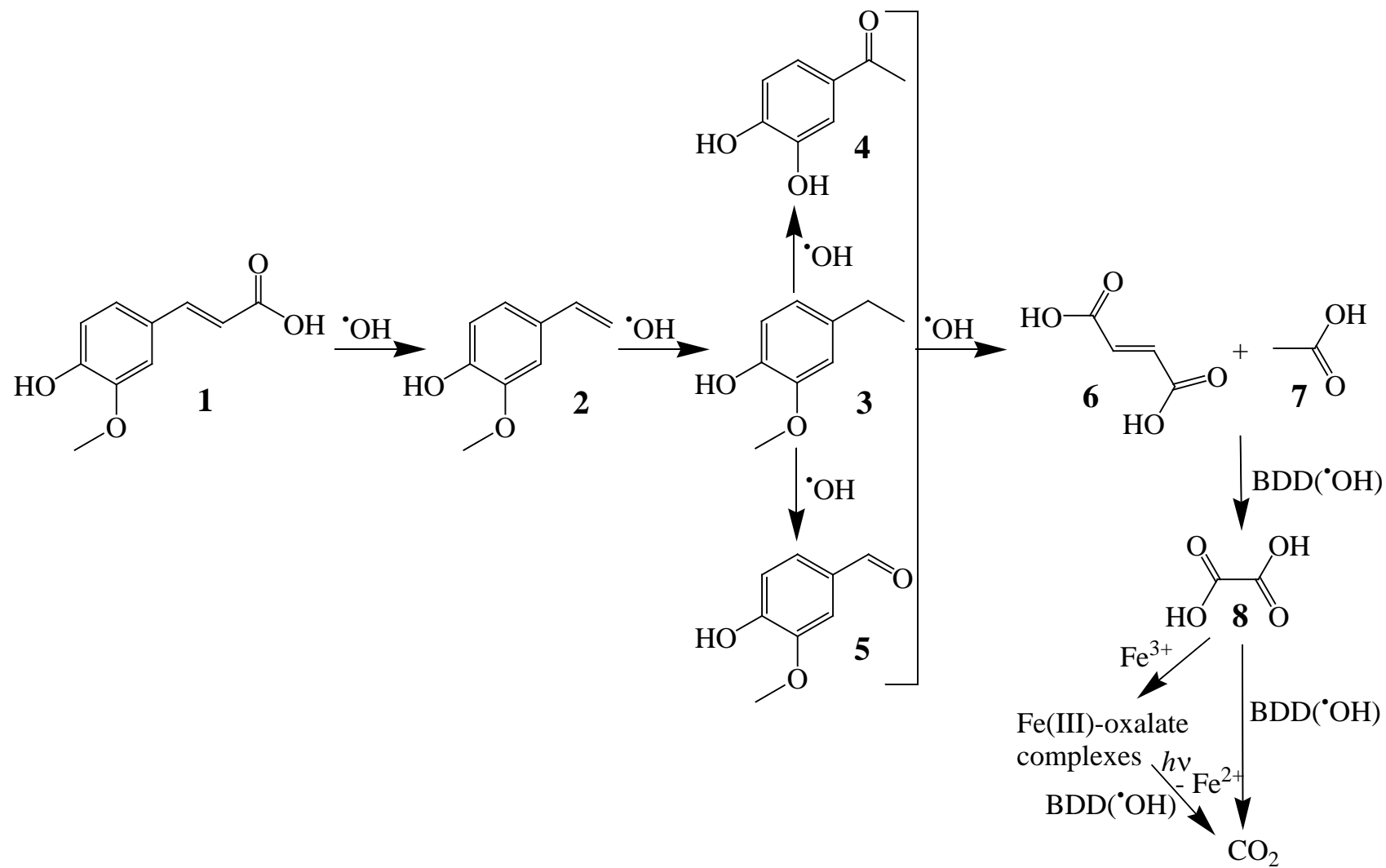


Fig. 7

Table 1.

Pseudo-first-order rate constant for *trans*-ferulic acid decay, along with its square regression coefficient, and percentage of TOC removed and mineralization current efficiency at 360 min determined for the degradation of 100 mL of solutions of this compound in 0.05 M Na₂SO₄ at pH 3.0 and 35 °C by electrochemical advanced oxidation methods using a stirred BDD/air-diffusion cell under different experimental conditions.

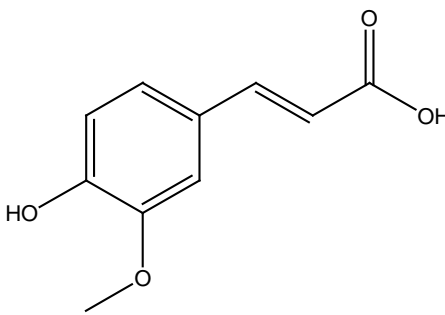
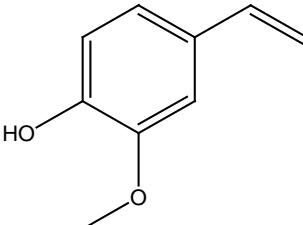
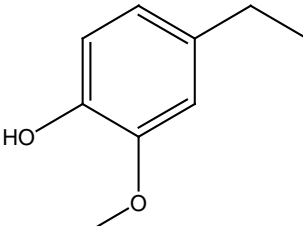
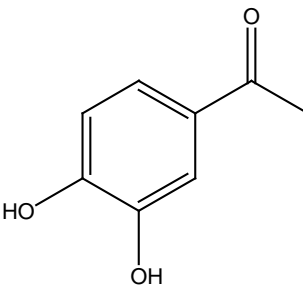
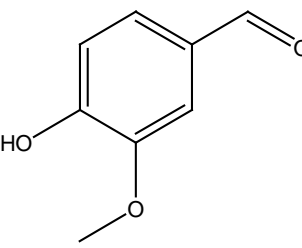
Method	[<i>trans</i> -ferulic acid] (mM)	Current density (mA cm ⁻²)	k_1 (min ⁻¹)	R^2	% TOC removed at 360 min	% MCE at 360 min	
AO-H ₂ O ₂	0.167	33.3	$(0.82 \pm 0.03) \times 10^{-2}$	0.993	74	2.3	
	0.417	33.3	$(0.74 \pm 0.03) \times 10^{-2}$	0.989	68	5.3	
	0.834	16.7				62	19
		33.3	$(0.72 \pm 0.01) \times 10^{-2}$	0.997	72	11	
		66.7				88	6.9
	100				94	4.9	
	1.668	33.3				67	21
EF ^a	0.167	33.3	0.87 ± 0.05	0.990	75	2.4	
	0.417	33.3	0.70 ± 0.04	0.993	77	6.0	
	0.834	16.7				74	23
		33.3	0.32 ± 0.02	0.990	80	13	
		66.7				87	6.7
	100				92	4.8	
	1.668	33.3				74	23
PEF ^b	0.167	33.3	0.88 ± 0.06	0.988	92	2.9	
	0.417	33.3	0.69 ± 0.03	0.993	94	7.3	
	0.834	16.7				98	31
		33.3	0.34 ± 0.02	0.991	98	15	
		66.7				98	7.7
	100				98	5.1	
	1.668	33.3				98	31

^a With addition of 0.50 mM Fe²⁺

^b With addition of 0.50 mM Fe²⁺ and irradiation with a 6 W UVA light ($\lambda_{\max} = 360$ nm).

Table 2.

Aromatic products identified by GC-MS during the electrolysis of 100 mL of a 0.834 mM *trans*-ferulic acid solution in 0.05 M Na₂SO₄ at pH 3.0 and 35 °C by AO-H₂O₂ using a stirred BDD/air-diffusion cell at 33.3 mA cm⁻².

Number	Name	Molecular structure	t_r (min)	m/z	Electrolysis time (min)
1	<i>trans</i> -Ferulic acid		33.9 ^a	194 (M ⁺), 179, 161, 133	30, 90
2	2-Methoxy-4-vinylphenol		20.1 ^a 31.3 ^b	150 (M ⁺), 135, 118, 107, 89, 77	30, 90 30, 90
3	4-Ethyl-2-methoxyphenol or 4-ethylguaiacol		28.1 ^b	152 (M ⁺), 137, 122, 109, 88	90
4	1-(2,4-Dihydroxyphenyl) ethanone		28.2 ^b	152 (M ⁺), 137, 123, 109, 81	30
5	Vanillin		23.2 ^a 37.5 ^b	152 (M ⁺), 151, 137, 123, 109, 81	90 30, 90

Retention times for: ^a non-polar Agilent J&W HP-5ms and ^b polar HP INNOWax columns.